VIII International Conference on Computational Methods for Coupled Problems in Science and Engineering
COUPLED PROBLEMS 2019
E. Oñate, M. Papadrakakis and B. Schrefler (Eds)

SURROGATE MODELS FOR THE ITERATIVE OPTIMUM-OPTIMORUM THEORY AND THEIR APPLICATIONS

A. NASTASE*

* Aerodynamics of Flight, RWTH, Aachen University
Templergraben 55, 52062 Aachen, Germany
email: nastase@lafaero.rwth-aachen.de

Key words: Surrogate Models, Coupled Viscous-Inviscid Flow, Iterative Global Shape Optimization, Aerospace Applications, Exploration of Supersonic Flow. .

Abstract. The author has developed non-classical three-dimensional hyperbolic analytic solutions (HASs) for the axial disturbance velocities over several flying configurations (FCs) in supersonic flow. The lift, pitching moment. inviscid drag coefficients and the distributions of pressure coefficients on FCs, at moderate angles of attack, can be rapid computed. The HASs are also used as start solutions for the design of inviscid, global optimized (GO) shapes of FCs, by using the own optimum-optimorum strategy. These inviscid GO shapes are proposed as surrogate models and are used in the first step of an iterative optimum-optimorum theory. Up the second step of iterations the HASs are replaced by hybrid analytic-numeric solutions for the Navier-Stokes layer and the friction drag coefficient is computed.

1 INTRODUCTION

The author uses the principle of minimal singularities of M. van Dyke, the compability conditions of P. Germain and the hydrodynamic analogy of E. Carafoli. for the development of non-classical three-dimensional HASs for the boundary valuue problems of hyperbolic PDEs of the axial disturbance velocities, over several FCs, in supersonic flow. These solutions are written in integrated forms and use mnimal singularities, which are located only along the singular lines (like subsonic leading edges, junction lines wing-fuselage, junction lines wing- leading edge flaps etc.) and fulfill the local jumps. These non-classical HASs are used in the first step of her iterative optimum-optimorum (IOO) strategy, as start solutions for the design of inviscid GO shapes of FCs. New performant FCs models with GO shapes are designed and tested in the trisonic wind tunnel of DLR Cologne. A new optimized variant of Saenger project for the touristic flight in space is proposed. The inviscid GO shapes of FCs are also used as surrogate models of IOO, in its first step of iteration. Up the second step of IOO, the use of hybrid analytic-numeric solutions for the PDEs of the three-dimensional Navier-Stokes layer (NSL) are proposed. These hybrid NSL's solutions use the HASs two time namely, as boundary values at the NSL's edge and to reinforce the NSL's solutions. These hybrid NSL's solutions which are products between the HASs and polynomes with free coefficients, have important analytic properties like: correct last behaviors, correct jumps over the singular lines. the singularities are balanced, the condition on the characteristic surfaces, which occurs in supersonic flow and the non-slip condition ares automatically fulfilled. A logarithmic density function is introduced instead of the density, in order to split the NSL's PDEs , as in [1] -]3]. The total drag of a FC, including friction, is computed.

2 THREE-DIMENSIONAL HYPERBOLIC POTENTIAL START SOLUTIONS FOR THE INVISCED, GLOBAL OPTIMIZATION

The author supposes that the downwashes of an FC are picewise given or approximate in form of superpositions of homogeneous polynomes in two variables and proposes some corresponding non-classical three-dimensional HASs for the axial disturbance velocities over the FCs, which are expressed in integrated forms and can be easy and rapid used: for the computation of the lift, pitching moment, inviscid drag coefficients and of the distributions of pressure coefficients over the FCs, as start solutions for the design of performant inviscid GO shapes of FCs, as outer flow for the Navier-Stokes layer (NSL) and for the generation of hybrid solutions.for the NSL, as in [1]-[4]. The HASs are presented here for three-dimensional FCs with arbitrary camber, twist and thickness distributions like delta wing alone and, delta wing fitted with central fuselage. Let us firstly introduce dimensionless coordinates

$$\tilde{x}_1 = \frac{x_1}{h_1} \quad , \quad \tilde{x}_2 = \frac{x_2}{\ell_1} \quad , \quad \tilde{x}_3 = \frac{x_3}{h_1} \quad , \qquad \text{(1a-c)}$$

$$\left(\tilde{y} = \frac{y}{\ell} \quad , \quad \ell = \frac{\ell_1}{h_1} \quad , \quad \nu = B\ell \quad , \quad B = \sqrt{M_\infty^2 - 1} \right) \quad ,$$

$$w = \tilde{w} \quad , \quad w^* = \tilde{w}^* \quad , \quad u = \ell\ \tilde{u} \quad , \quad u^* = \ell\ \tilde{u}^*$$

Hereby u and $u^\bullet$ and w and $w^\bullet$ are the axial disturbance velocities and the downwashes on the thin and thick-symmetrical wing components ℓ_1, h_1 and ℓ are the half-span, maximal depth and the dimensionless span and ν is the similarity parameter of the planform.

Let us consider firstly the delta wing alone. The distributions of the downwashes w and w^* on the thin and thick-symmetrical components of the thick, lifting delta wing are the following :

$$w \equiv \tilde{w} = \sum_{m=1}^{N} \tilde{x}_1^{m-1} \sum_{k=0}^{m-1} \tilde{w}_{m-k-1,k} \left|\tilde{y}\right|^k \quad , \quad w^* \equiv \tilde{w}^* = \sum_{m=1}^{N} \tilde{x}_1^{m-1} \sum_{k=0}^{m-1} \tilde{w}^*_{m-k-1,k} \left|\tilde{y}\right|^k \qquad \text{(2a, b)}$$

The corresponding axial disturbance velocities on the thin and on the thick components fitted with a central ridge, are :

$$u \equiv \ell\ \tilde{u} = \ell \sum_{n=1}^{N} \tilde{x}_1^{n-1} \left\{ \sum_{q=0}^{E\left(\frac{n}{2}\right)} \frac{\tilde{A}_{n,2q}\tilde{y}^{2q}}{\sqrt{1-\tilde{y}^2}} + \sum_{q=1}^{E\left(\frac{n-1}{2}\right)} \tilde{C}_{n,2q}\tilde{y}^{2q} \cosh^{-1} \sqrt{\frac{1}{\tilde{y}^2}} \right\}$$

$$u^{*} \equiv \ell\ \tilde{u}^{*} = \ell \sum_{n=1}^{N} \tilde{x}_1^{n-1} \left\{ \sum_{q=0}^{n-1} \tilde{H}^{*}_{nq} \tilde{y}^{q} \left(\cosh^{-1} M_1 + (-1)^q \cosh^{-1} M_2 \right) \right.$$

$$\left. + \sum_{q=1}^{E\left(\frac{n-1}{2}\right)} \tilde{C}^{*}_{n,2q} \tilde{y}^{2q} \cosh^{-1} \sqrt{\frac{1}{\nu^2 \tilde{y}^2}} + \sum_{q=0}^{E\left(\frac{n-2}{2}\right)} \tilde{D}^{*}_{n,2q} \tilde{y}^{2q} \sqrt{1-\nu^2 \tilde{y}^2} \right\} , \qquad \text{(3a, b)}$$

$$\left(M_1 = \sqrt{\frac{(1+\nu)\,(1-\nu\ \tilde{y})}{2\nu(1-\tilde{y})}} , \qquad M_2 = \sqrt{\frac{(1+\nu)\,(1+\nu\ \tilde{y})}{2\nu(1+\tilde{y})}} \right) ,$$

The coeficients of the axial disturbance velocity are linear and homogeneous functions of the coefficients of the downwashes , it is :

$$\tilde{A}_{n,2q} = \sum_{j=0}^{n-1} \tilde{a}_{n,2q,j}\ \tilde{w}_{n-j-1,j} , \qquad \tilde{C}_{n,2q} = \sum_{j=0}^{n-1} \tilde{c}_{n,2q,j}\ \tilde{w}_{n-j-1,j} ,$$

$$\tilde{H}^{*}_{nq} = \sum_{j=0}^{n-1} \tilde{h}^{*}_{n,q,j}\ \tilde{w}^{*}_{n-j-1,j} , \qquad \tilde{C}^{*}_{n,2q} = \sum_{j=0}^{n-1} \tilde{c}^{*}_{n,2q,j}\ \tilde{w}^{*}_{n-j-1,j} ,$$

$$\tilde{D}^{*}_{n,2q} = \sum_{j=0}^{n-1} \tilde{d}^{*}_{n,2q,j}\ \tilde{w}^{*}_{n-j-1,j} \qquad \text{(4a-e)}$$

If the delta wing fitted with a central fuselage is now treated, this FC is considered as a discontinous wing fitted with two artificial ridges along the junction lines wing-fuselage.

The downwashes on the thin and thick-symmetrical wing components of FC are given, as in (1a, b) and, of the non-integrated central fuselage zone, are given or approximate in the following forms:

$$w' \equiv \overline{w} = \sum_{m=1}^{N} \tilde{x}_1^{m-1} \sum_{k=0}^{m-1} \overline{w}_{m-k-1,k} |\tilde{y}|^{k} , \qquad w'^{*} \equiv \overline{w}^{*} = \sum_{m=1}^{N} \tilde{x}_1^{m-1} \sum_{k=0}^{m-1} \overline{w}^{*}_{m-k-1,k} |\tilde{y}|^{k} , \qquad \text{(5a, b)}$$

The corresponding axial disturbance velocities on the components of the non-integrated wing-fuselage FC are, as in [1], it is:

$$u \equiv \ell\ \tilde{u} = \ell \sum_{n=1}^{N} \tilde{x}_1^{n-1} \left\{ \sum_{q=0}^{n-1} \tilde{G}_{nq}\ \tilde{y}^{q} \left(\cosh^{-1} S'_1 + (-1)^q \cosh^{-1} S'_2 \right) \right.$$

$$+\sum_{q=0}^{E\left(\frac{n}{2}\right)} \frac{\widetilde{A}_{n,2q}\ \widetilde{y}^{2q}}{\sqrt{1-\widetilde{y}^2}} + \sum_{q=1}^{E\left(\frac{n-1}{2}\right)} \widetilde{C}_{n,2q}\ \widetilde{y}^{2q} \cosh^{-1}\sqrt{\frac{1}{\widetilde{y}^2}} \ \Bigg\} \quad ,$$

$$\left(S_1' = \sqrt{\frac{(1+\bar{\nu})\,(1-\widetilde{y})}{2\,(\bar{\nu}-\nu\,\widetilde{y})}} \quad , \quad S_2' = \sqrt{\frac{(1+\bar{\nu})\,(1+\widetilde{y})}{2\,(\bar{\nu}-\nu\,\widetilde{y})}} \right)$$

$$u'^{*} \equiv \ell\ \widetilde{u}'^{*} = \ell \sum_{n=1}^{N} \widetilde{x}_1^{n-1} \Bigg\{ \sum_{q=0}^{n-1} \widetilde{H}^{*}_{nq}\ \widetilde{y}^{q} \left(\cosh^{-1} M_1 + (-1)^q \cosh^{-1} M_2 \right)$$

$$+ \sum_{q=0}^{E\left(\frac{n-2}{2}\right)} \widetilde{D}^{*}_{n,2q}\ \widetilde{y}^{2q} \sqrt{1-\nu^2\widetilde{y}^2} + \sum_{q=1}^{E\left(\frac{n-1}{2}\right)} \widetilde{C}^{*}_{n,2q}\ \widetilde{y}^{2q} \cosh^{-1}\sqrt{\frac{1}{\nu^2\widetilde{y}^2}}$$

$$+ \sum_{q=0}^{n-1} \widetilde{G}^{*}_{nq}\ \widetilde{y}^{q} \left(\cosh^{-1} S_1 + (-1)^q \cosh^{-1} S_2 \right) \Bigg\} \quad , \qquad \text{(6a, b)}$$

$$\left(S_1 = \sqrt{\frac{(1+\bar{\nu})\,(1-\nu\,\widetilde{y})}{2\,(\bar{\nu}-\nu\,\widetilde{y})}} \quad , \quad S_2 = \sqrt{\frac{(1+\bar{\nu})\,(1+\nu\,\widetilde{y})}{2\,(\bar{\nu}+\nu\,\widetilde{y})}} \quad c = \frac{c_1}{h_1} \quad , \quad \bar{\nu} = Bc \right),$$

Hereby c_1 and c are the half-span, and the dimensionless span and $\bar{\nu}$ is the similarity parameter of the planform of the fuselage. The coefficients of axial disturbance velocity are linear and homogeneous functions of the coefficients of the downwashes , it is :

$$\widetilde{A}_{n,2q} = \sum_{j=0}^{n-1} \left(\widetilde{a}_{n,2q,j}\widetilde{w}_{n-j-1,j} + \bar{a}_{n,2q,j}\bar{w}_{n-j-1,j} \right) \quad , \qquad \widetilde{C}_{n,2q} = \sum_{j=0}^{n-1} \bar{c}_{n,2q,j}\bar{w}_{n-j-1,j} \quad ,$$

$$\widetilde{G}_{nq} = \sum_{j=0}^{n-1} \left(\widetilde{g}_{n,q,j}\widetilde{w}_{n-j-1,j} + \bar{g}_{n,q,j}\bar{w}_{n-j-1,j} \right)$$

$$\widetilde{H}^{*}_{nq} = \sum_{j=0}^{n-1} \widetilde{h}^{*}_{n,q,j}\widetilde{w}^{*}_{n-j-1,j} \quad , \qquad \widetilde{C}^{*}_{n,2q} = \sum_{j=0}^{n-1} \bar{c}^{*}_{n,2q,j}\bar{w}^{*}_{n-j-1,j} \quad ,$$

$$\widetilde{D}^{*}_{n,2q} = \sum_{j=0}^{n-1} \left(\widetilde{d}^{*}_{n,2q,j}\widetilde{w}^{*}_{n-j-1,j} + \bar{d}^{*}_{n,2q,j}\bar{w}^{*}_{n-j-1,j} \right) \quad ,$$

$$\widetilde{G}^*_{nq} = \sum_{j=0}^{n-1} \left(\widetilde{g}^*_{n,q,j} \widetilde{w}^*_{n-j-1,j} + \overline{g}^*_{n,q,j} \overline{w}^*_{n-j-1,j} \right) \tag{7a-g}$$

The integrated wing-fuselage FC, considered for the desigm of GO FC's shape, has continous mean surface and the same tangent planes along the junction lines wing-fuselage, in order to avoid the corners. The corresponding axial disturbanve velocity of its thin component has the form (3a). Now the HAS are further used as start solutions for the design of GO shape of integrated wing-fuselage FCs.

3 INVISCID, GLOBAL OPTIMIZED SHAPES OF FLYING CONFIGURATIONS

The free parameters of the design of the inviscid GO shape of the integrated wing-fuselage FC are the coefficients öf the downwashes w , $w^{\bullet}$, $w'^{\bullet}$,

The constraints for the thin component of FC are the following: given lift and pitching moment coefficients and the Kutta condition along the subsonic leading edges, in order to avoid the conturnement of the flow, at cruise. The constraints for the thick-symmetrical component of FC are: given relative volumes of the wing and of the fuselage zone and the integration conditions along the junction lines wing-fuselage in order to avoid the corners on the FC's surface. The design of the GO shape of an integrated wing-fuselage FC leads to an enlarged variational problem with free boundaries. The author has developed an enlarged variational strategy called optimum-optimorum strategy, as in [1]-[4], in order to solve this enlarged variational problem. The separate treatment of the variational problems of the thin and thick-symmetrical components lead to the solving of two linear algebraic systems for the determination of the best values of the coefficients of the downwashes. But these systems are coupled, due to their common similarity parameters, which enter in the coefficients of these systems and which must be also, simoultanieously be optimized. Due to the fact that the quotient of the similarity parameters of the planforms of the wing and of the fuselage are determined for the purpose of the FC, this quotient is taken constant during the optimization process and the similarity parameter of the wing with subsonic leading edges is sequentially varied between 0 and 1. A lower limit line of the drag coefficients of elitary FCs, as function of the similarity parameter of the planform of the wing is obtained and the position of the minimum of this limit line is the optimal value of the similarity parameter of the planform of the wing and the corresponding elitary wing is in the same time the GO shape of the FC. Three GO models, namely ADELA, a wing alone and two GO shapes of the fully-integrated wing-fuselage FCs, namely FADET I and FADET II were designed by the author, for the cruising Mach numbers 2 , 2.2 and, respectively, 3.

A theoretical and experimental exploration of supersonic flow over FCs was performed by using eight models designed by the author, namely: a wedged delta wing, a double wedged delta wing, a wedged delta wing fitted with a central conical fuselage,a GO delta wing alone ADELA, global optimized at cruising Mach number $M_\infty = 2$, a wedged rectangular wing and a cambered rectangular wing, are presented in the (Fig.1). In the (Fig.2) are presented two, more recent designed and experimental cheked GO models of fully-integrated wing-fuselage

FCs FADET I and FADET II; global optimized at $M_\infty = 2.2$ and, respectively, at $M_\infty = 3.$ All these models have sharp leading edges in order to avoid the bow shock wave. The six delta FCs have the same area of their planforms and the both rectangular wings have the same planforms The three global optimized flying configurations fulfill additionally the Kutta condition along their subsonic leading edges, in order to avoid the detachment of the flow along their leading edges, to concel the induced drag and to increase the lift.

The measurements of the lift, pitching moment and pressure coefficients on the upper side of these models were performed in the trisonic wind tunnel of DLR Cologne, in the frame of research projects of the author, sponsored by the DFG. Correlation and interpolation software, developed by the author, were used by herself and by her young collaborators of Aerodynamics of Flight, at RWTH, Aachen University, for the evaluation and for the plotting of these experimental results. The theoretical predicted pressure, lift and pitching moment coefficients are obtained by using the non-classical three-dimensional hyperbolic potential solutions and the corresponding software of the author.

Fig. 1 Six of the models used for the exploration of supersonic flow

Fig. 2 The fully-integrated and global optimized models FADET I and FADET II

A very good agreement between the theoretical and experimental correlated values of lift and pitching moment coefficients are obtained for all the range of supersonic Mach numbers and for the angles of attack $\alpha \leq 20^{\circ}$ For the pressure coefficients a good agreement between the theoretical and the experimental results is obtained for the angles of attack $\alpha \leq 10^{\circ}$

The agreement between the experimental and theoretical HASsfor the pressure, lift and pitching moment of flattened FCs flying at moderate angles of attack, leads to the following important conclusions:

- the flow is laminar, as supposed here, and it remains attached in supersonic flow, for larger range of angles of attack than by subsonic flow;
- the flight with characteristic surface, which is more economic, instead of the flight with shock wave surface is confirmed;
- the validity of the three-dimensional hyperbolic analytic potential solutions for the axial disturbance velocity, with the chosen balanced minimal singularities and the corresponding developed software for the computation of the above coefficients are confirmed;
- the influence of friction upon these coefficients is neglectable;
- these analytic solutions are very usefull for the computation of proposed hybrid solutions for the NSL's PDEs, which are able to compute the total drag, including friction ;

4 AEROSPACE APPLICATIONS

The designed GO shapes of FCs are used as sources of inspirations for the design of new, almost blended and high performant shapes of new generation of models of supersonic aircraft, aerospace vehicles and supersonic UAVs . One application, presented here, is related with a suborbital touristic flight in space. New GO shapes of vehicles models GEO and LEO, optimized at cruising Mach numbers $M_{\infty} = 2.2$ and respectively $M_{\infty} = 3.$, with two congruent fuselages, only almost inserted in the wing's thickness (in order to have windows on both sides!) and converging in the frontal part of the wing, are here proposed , as in the (Fig. 3) and (Fig. 4). GEO with a GO shape is a greater model for geostationary vehicle and a smaller one, LEO, with its GO shape, is the model for the lower earth orbit vehicle. A variant of Saenger project now with two GO space vehicles is here proposed for the touristic flight in space. The vehicle GEO can carry the smaller vehicle LEO, as presented in the (Fig. 5) during the change of passengers and for supply. LEO can up and go on GEO . During the flight of LEO in space, different UAVs can up and go from earth on GEO, for supply and exchange of passengers.

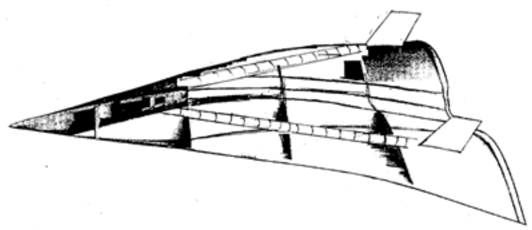

Fig. 4 The greater fully-integrated and global optimized model of space vehicle GEO

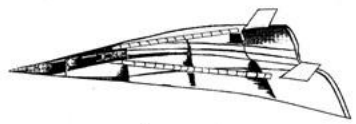

Fig. 5 The smaller, fully-integrated and global optimized modelof space vehicle LEO

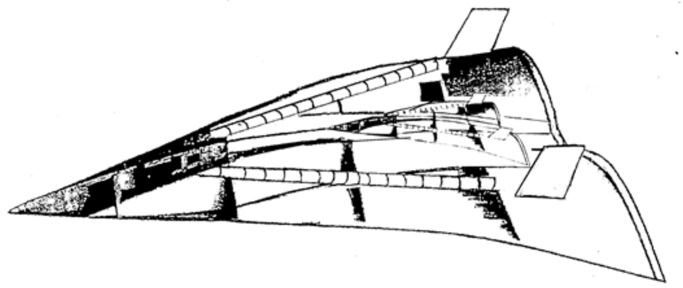

Fig. 6 GEO carrying LEO

5 HYBRID SOLUTIONS FOR THE NAVIER-STOKES LAYER.

The proposed hybrid analytic-numeric solutioms for the NSL use the non-classical HASs two times, it is: as outer flow as the NSL's edge and to reinforce the numerical NSL's solutions. Let us firstly introduce the coordinate η inside the NSL, it is

$$\eta = \frac{x_3 - Z(x_1,\ x_2)}{\delta(x_1,\ x_2)} \qquad (0 \le \eta \le 1) \qquad (8)$$

The proposed hybrid solutions for the velocity components, the here introduced density function $R = \ln \rho$ and of the absolute temperature T are the following:

$$u_\delta = u_e \sum_{i=1}^{N} u_i\, \eta^i \quad , \qquad v_\delta = v_e \sum_{i=1}^{N} v_i\, \eta^i \quad , \qquad w_\delta = w_e \sum_{i=1}^{N} w_i\, \eta^i \qquad (9a,\ b.\ c)$$

$$R = R_w + (R_e - R_w) \sum_{i=1}^{N} r_i\, \eta^i \qquad T = T_w + (T_e - T_w) \sum_{i=1}^{N} t_i\, \eta^i \qquad (10a,\ b)$$

Hereby are: δ the thickness of the NSL, u_e , v_e , w_e the velocity components of the hyperbolic potential flow at the NSL's edge, R_e and T_e the density function and the absolute temperature of the outer flow at the NSL's edge and R_w and T_w their values at the surface of the FC. The free coefficients r_i , t_i , u_i , v_i , w_i are used to satisfy the NSL's PDEs and the boundary conditions at the NSL's edge in some points. The viscosity μ fulfills an exponential low and the pressure p is obtained from the physical equation of the ideal gas, it is

$$\mu = \mu_{\infty} \left(\frac{T}{T_{\infty}} \right)^{n_1} \quad , \qquad p = R_g \, \rho \, T = R_g \, e^R \, T \qquad \text{(11a, b)}$$

All the physical entitis are expressed as functions of the velocity's coefficients, which are determined by using the collocation method and by iterative solving of the impulse PDEs .The skin friction, the friction drag and the total drag coefficients of a delta wing are the following:

$$\tau_{x_1}^{(w)} \equiv \tau_{x_1} \Big|_{\eta = 0} = \mu_f \frac{\partial u_\delta}{\partial \eta} \Big|_{\eta = 0} = \mu_f u_1 u_e \ , \qquad (12)$$

$$C_d^{(f)} = 8 \int_{\tilde{O}\tilde{A}_1\tilde{C}} \nu_f \, u_1 \, u_e \, \tilde{x}_1 \, d\tilde{x}_1 \, d\tilde{y} \quad , \qquad C_d^{(t)} = C_d^{(f)} + C_d^{(i)}$$

6 CONCLUSIONS

- The use of HASs as start solutions allow the rapid inviscid design of GO shapes of performant FCs, which are here proposed for the shapes of aerospace vehicles and as surrogate models for the IOO.
- The use of surrogate models speed up the computation time for the design of GO shapes of the FCs and are used in the first step of an iterative optimum-optimorum strategy, as in [1]-[4].
- The HASs are also used two times for the determination of hybrid solutions for the Navier-Stokes layer it is, as boundary at the NSL's edge and in the structure of hybrid solutions, which are products of HASs with polynomes with free coefficients. These coefficients are used to satisfy the NSLs PDEs in a number of points.
- The hybrid NSL's solutions replace the HASs up the second step of IOO and allow the computation of total drag, including friction.

5 REFERENCES

[1] Nastase, A. C*omputation of supersonic flow.over flying configurations*, Elsevier, Oxford, UK , (2008).

[2] Nastase, A, Hybrid Navier-Stokes solutions for aerodynamical global optimal shape's design, *Proc. EngOpt, Paper 750, Rio de Janeiro, Brazil* (2008) .

[3] Nastase, A. Evolutionary iterative optimum-optimorum theory, *INCAS Bulletin Bucharest Romania,* Vol. 2, Number 4, (2010), p. 153-161

[4] Nastase, A. Theoretical and experimental exploration of supersonic flow (part 1), *Proc. of 'Aerospatial 2016', Bucharest, Romania,* (2017), p. 3-21